A NOVEL SINGLE-STAGE LIGHT EMITTING DIODE DRIVER FOR STREET-LIGHTING APPLICATIONS WITH POWER FACTOR CORRECTIONS

Y Prasanna Krishna[1] | G Ravindra Reddy[2] | V Suresh[3]

[1](Department of EEE, P.G Student, PINN, Nellore, A.P, India, yathapalliprasanakrishna@gmail.com)

[2](Department of EEE, Assistant Professor, PINN, Nellore, A.P, India, ravigopireddy51@gmail.com)

[3](Department of EEE, Research Scholar, SVCET, Chittoor, A.P, India, sureshvendoti@gmail.com)

Abstract— *In this paper, a novel single-stage light emitting diode (LED) driver for street lighting applications with power factor corrections (PFC) is proposed. The presented driver integrates a customized bridgeless PFC ac-dc converter with a half-bridge type LLC dc-dc resonant converter into a single-stage conversion circuit topology. The proposed ac-dc resonant driver provides input current shaping, and it offers quality of lowered switching losses to the soft-switching functions obtained on two power switches and two output-rectifier diodes. The proposed model is designed and simulated in software called MATLAB/SIMULATION and the results shows that the performance of the novel single stage light emitting diode driver.*

Keywords—Light emitting diode (LED);Power factor correction (PFC);Street lighting;Matlab Simulation Results

1. INTRODUCTION

Light Emitting diodes (LEDs) have favorable features of smaller size, longer lifetime, lower maintenance costs, greater strength against breakage, and being mercury free and therefore less harmful to our environment than traditional lighting sources [1] and [8]. Thus, LEDs have become increasingly common in our daily lives. They are well suited to indoor and outdoor energy-saving lighting applications, such as traffic lighting, background lighting, displays, street lighting, automotive and motorcycle lighting, decorative lighting, and so on.

TABLE 1: COMPARISONS BETWEEN TRADITIONAL AND NEW LIGHTING SOURCES STREET-LIGHTING APPLICATIONS.

Items	Traditional	New
Lighting Source	High Pressure Sodium Lamp	LED
Lamp Model	OSRAM NAV-E 150	AcBel LM9003-003 G/GT
Power Consumption	150W	157.3W
Output Luminous Flux	14500 lm	12000 lm
Luminous Efficacy	97 lm/W	83 lm/W
Color Temperature	2000 K	5000–6300 K
Color Rendering Index (CRI)	≤25	70
Lamp Life	> 24000 hours	> 50000 hours

The installation of street lights is closely related to the development of one area or region, and they represent the financial success of a city. For street-lighting applications, the traditional lighting sources are high-intensity-discharge (HID) lamps, such as high-pressure sodium lamps and high-pressure mercury lamps. Recently, LEDs are commonly being used as new sources for street-lighting applications due to their attractive characteristics of good color rendering index, energy-savings being mercury free, quickly turning ON and OFF, that they do not require a high striking voltage for starting the lamp up and an extra-high ignition voltage in the hot restart status, and that they offer a long-life time in comparison to their traditional counter parts.

The customary lighting source is a high-weight sodium light, (for example, a 150 W osram nav-e light), and the new one is a LED light (a 144 W AcBel lm 9003-003 g/gt light [22] for instance) as an option choice for road lighting conditions. As appeared in table-1,the LED light expends less power and has better shading rendering file and longer light life than the customary one. Rather than customary hid lighting sources, for example, high-weight sodium lights and high-weight mercury lights, led, which offers elements of fulfilling lighting effectiveness, diminished power utilization, and long lifetime, will assume an imperative part for road light applications later on.

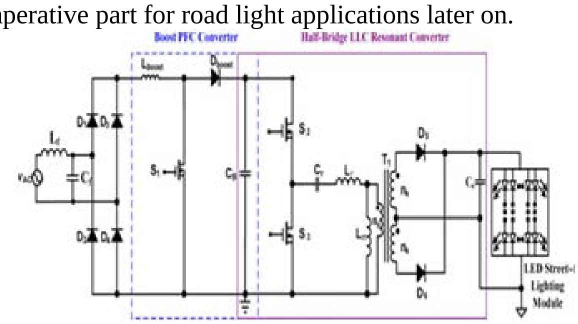

Fig.1: Conventional two-organize driver for providing a LED road lighting module.

The traditional confined driver for fueling a led road lighting module with an evaluated light force of more noteworthy than 70 WI’s a two-organize topology [16], as appeared in fig.1, and comprises of a help control calculate rectification (PFC) dc–dc converter (counting an inductor boost) a power switch S1, a diode (boost) and a dc-connected capacitor Cb) for information current forming, and a half-connect sort LLC dc–dc resounding converter (counting a dc-connected capacitor Cb , two power switches S2 and S3 , a resonant capacitor Cr, an inductor, an inside tapped transformer with two yield windings, two yield diodes D5 and D6, and a capacitor) for fueling the led road lighting module.

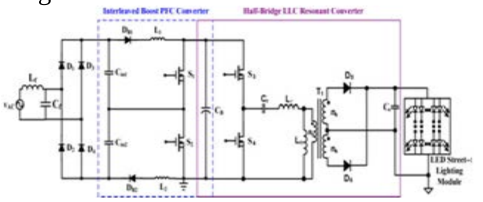

Fig.2: Another customary two-stage driver for providing a LED road lighting module.

The fig-2 demonstrates another customary two-stage disconnected driver for providing a led road lighting module with an evaluated force of bigger than 70w; this rendition comprises of an interleaved support PFC ac–dc converter (counting two capacitors Cin1 and Cin2, two diodes DB1 and DB2, two inductors L1 andL2, two power switches S1 and S2and a dc-connected capacitor (CB) and a half-connect sort LLC dc–dc thunderous converter for fueling the road lighting module. These customary led drivers are reasonable for working in a wide information utility-line voltage run (for instance, from 85 to 265 Vac), and the voltage crosswise over the dc-connected capacitor can be controlled. Be that as it May, more power switches and segments are required in these conventional drivers, and the circuit effectiveness is restricted because of the two-arrange control change. Because of these difficulties, this paper displays a novel single-stage high-proficiency financially savvy driver with PFC for providing a led road lighting module, and the proposed driver is reasonable for working in American scope of utility-line voltage (from 90 to 130 Vac).

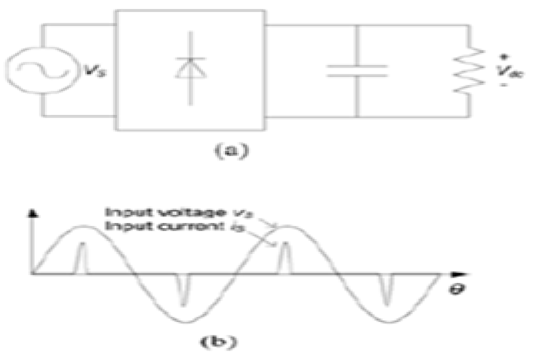

Fig. 3: (a) Diode rectifier with a capacitor associated at the dc yield side. (b) Input voltage and current waveforms.

Developing advancements, for example, remote power exchange (WPT) frequently embrace a high working recurrence in the range from a couple of hundred of KHZ to more than 10 MHZ recently, much research exertion has been given to enhancing the execution of WPT frameworks as far as exchange separation and framework's vitality effectiveness there is an absence of research focusing on the ideal outline of the power converter at the recipient side. Generally, the most straightforward approach is to utilize a diode rectifier circuit with a yield stockpiling capacitor, as appeared in fig. 3(a). Nonetheless, this capacitor is charged to esteem near the pinnacle of the air conditioner input voltage.

Subsequently, throbbing info current of expansive extent happens close to the pinnacle of the air conditioner input voltage. Spasmodic current infers that remote power does not stream ceaselessly from the essential side of the WPT framework to the yield of the framework. Such diode rectifiers draw very misshaped current from the air conditioner control source and result in a poor information control calculate (PF). The vitality effectiveness and power exchange ability of a poor PF framework are moderately low due to the high conduction misfortune in the influence converters and transmission wires. Moreover, the twisted current has a rich high-arrange consonant substance which may cause the discharge of electromagnetic impedance (EMI) that influences the operation of neighbor electronic hardware.

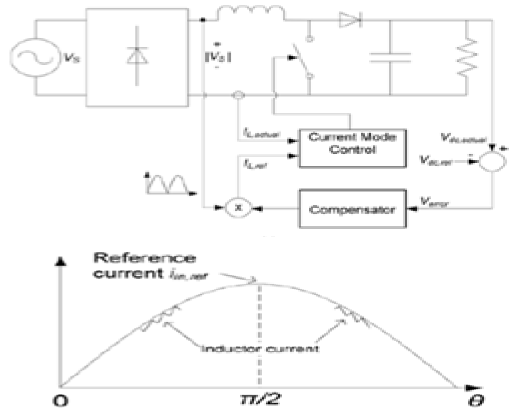

Fig.4: (a) PF correction circuit. (b) Input voltage and Current waveforms

A power electronic converter, for example, a help converter can be utilized to shape the information air conditioning current attracted by the rectifier to be sinusoidal and in stage with the air conditioner voltage. Fig.4 (a) demonstrates a traditional support converter associated after a diode connect rectifier to frame a PF remedy (PFC) circuit. The yield dc voltage is detected and sustained to a blunder speaker. The contrast between the real and reference voltage is determined and connected to a compensator circuit, for example, a corresponding basic (pi) compensator. The yield of the compensator is duplicated with the flag relative to the air conditioner voltage waveforms Vsto create the reference current flag iLref. Subsequently, a present mode controller is utilized to create the on and off flag to the switch molding the present waveform of the inductor. In this way, the normal of the air conditioner current is compelled to take after the waveform of the air conditioner voltage.

Fig.4 (b) portrays the information air conditioning current waveform of the converter. It can be watched that the exchanging recurrence of the PFC converter must be a few times higher than the recurrence of the air conditioner framework. Utilizing a 400-khz air conditioning transmission framework for instance, applying this present molding innovation suggests that the power change needs to work in the several MHZ accordingly, the exchanging misfortune gets to be noteworthy and the proficiency of the converter pointedly decreases.

Beforehand a solitary stage light transmitting diode led driver with interleaving power-calculate rectification (PFC) highlights for road lighting applications. The exhibited circuit incorporates an entomb leaved help PFC converter with a half-connect sort LLC thunderous converter into a solitary stage control converter. The displayed ac-dc full converter utilizes interleaving techniques to accomplish input-current molding, and has delicate exchanging capacities on two dynamic power changes to diminish their exchanging misfortunes keeping in mind the end goal to expand the circuit effectiveness. The proposed led driver highlights low levels of information ebb and flow swell, diminished exchanging misfortunes, high influence figure, low aggregate sounds contortion (THD) of info ebb and flow, and a decreased parts number.

The paper is sorted out as takes after. In further area, the idea of utilizing inductor capacitor (Lc) arrangement full circuit to perform PF revision will be presented. The working rule of the proposed high-recurrence nourished air conditioning dc control converter will be expressly portrayed utilizing the comparing timing graphs and identical circuit charts. At that point, the voltage change proportion and productivity of the converter will be diagnostically examined and displayed. Thereafter, the development of a proof of idea model and its test estimation results will be examined.

2. ANALYSIS OF THE PROPOSED SINGLE STAGE LED DRIVER

The proposed driver for fueling a led road lighting module with an appraised led force of bigger than 70 W is displayed in fig. 5 as appeared, it consolidates a changed bridgeless ac-dc converter with a half-connect sort LLC dc-dc resounding converter into a solitary phase of force transformation. The single-stage driver comprises of a channel inductor Lf, a channel capacitor Cf an inductor Lb, two diodesD1 and D2, two power switches S1 and S2, a dc-connected capacitor CB, a thunderous capacitor Cr, an inductor Lr, an inside tapped transformer T1 with two yield windings, two diodes D3 and D4 and a capacitor, Co along with the led road lighting module. Fig.5 likewise demonstrates the piece chart for controlling the single-stage led driver, and the introduced control circuit is appeared in fig. 6 Alluding to the fig 6 and fig 7 a consistent voltage and steady Ebb and flow (Cv–Cc) controller (IC1 SEA05) is embraced to detect the yield voltage through resistors Rvs1 and Rvs 2, while all the while detecting the yield ebb and flow through the resistor R Cs for providing the evaluated voltage and ebb and flow to the exploratory led road lighting module.

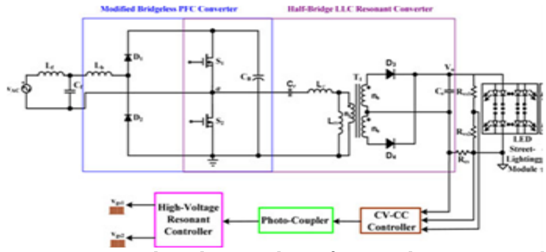

Fig. 5: Proposed single-stage driver for providing a LED road-lighting module.

The yield flag of the Cv–Cc controller sustains into the high-voltage resounding controller (IC3 l6599) through a photograph coupler (IC2 pc817). Two entryway driving signs Vgs1 and Vgs2generating from the full controller direct the yield voltage and current of the led road lighting module by utilizing variable-recurrence control conspire. In addition, the inductor L1 is intended to be worked at intermittent conduction mode(DCM) for actually accomplishing PFC in expansion, the proposed led driver spares three diodes and one control switch contrasted and the traditional two-organize driver appeared in fig. 1. Additionally, the proposed driver conserves on segments tally (barring four diodes, two capacitors, two power switches and an inductor) interestingly with the two-organize driver appeared in fig. 2.

Keeping in mind the end goal to dissect the exhibited single-stage led road lighting driver, a few suppositions are made, recorded as takes after:

Control switches S1 and S2 are integrally worked, and their inborn capacitors and diodes are considered.

The LC input channel is not appeared in the circuit while dissecting the operational methods of the led driver.

The directing voltage drops and proportional resistors of yield corrected diodes D3and D4are over looked.

The inductor Lb is intended to be worked in DCM.

The recurrence of the two power switches is much higher than that of the utility-line voltage, so amid investigation the utility-line voltage can be dealt with as a steady esteem in every exchanging period.

Fig.5 presents the improved single-stage led driver for providing the road lighting module used to examine the operational modes for the positive utility-line half-cycle (the examination for the negative one is comparative).

The info utility-line voltage v_ACis characterized as,

$$v_{AC}(t) = \sqrt{2v_{AC-rms} \sin 2\pi f_{AC} t}\ \text{n} \qquad (1)$$

Where

v_{AC-rms} is the root-mean-square (rms) estimation of the input voltage, and f_{AC} is the utility-line recurrence.

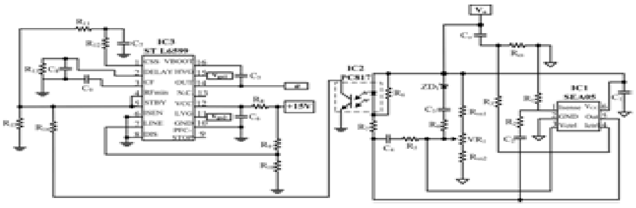

Fig. 6: Presented control circuit of the single-stage LED driver.

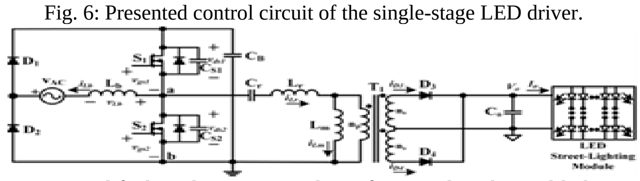

Fig. 7: Simplified single-stage LED driver for providing the road-lighting module a mid examination of the operational modes.

Figs. 6 and 7 individually, exhibit the operational modes and standard waveforms of the proposed single-stage driver for providing a led road lighting module. What's more, Cs1 and Cs2 are the characteristic capacitors of switches S1 and S2, Lm the attractive inductor of the transformer T1, iLbis the current of inductor Lb. iLr is the resounding inductor current, and iLm is the attractive inductor current. The examination and depictions for each operational mode are recorded as takes after.

Mode 1 [t_0≤t<t_3; see Fig. 8(a)]:

At the point when $vds1$ declines to zero at time instantt_0 , this mode starts. The power switch S_1 turns ON with zero-voltage switching (ZVS). The utility-linevoltage v_{Ac}charges the inductor $L_b$through the diodeD_1. Theinductor current i_{Lb}linearly increments, and it is given by

$$i_{Lb}(t) = \frac{v_{AC}(t)}{L_b} t \qquad (2)$$

The inductors Lm and Lr provide vitality to Cr and CB through the body diode of S, and to capacitor C0 alongside the led road lighting module through diodeD3. At time instant t1, the inductor current i(Lr) becomes zero. Moreover, the dc linked capacitor CB provides vitality to Cr and Lr through the switch S1, and the attractive inductor Lm provides vitality to the capacitor C0 along with the LED road lighting module through diode D3. At time, moment t, the inductor current i (Lm) increases to zero. In addition, the dc-linked capacitor CB provides energy to Cr, Lr and Lm through the switch S1, and to the capacitor C0 along with the LED road-lighting module through diode D_3. When I D_3 declines to zero, Mode-1 closes.

Mode 2 [t_3≤t<t_4; see Fig. 8(b)]:

At t3, the utility-line voltage Vac still charges the inductor Lb through the diode D1. Current i(Lb) reaches its most extreme values i(Lb-pk) (t), and can be expressed as,

$$i_{Lb-pk}(t) = \frac{v_{AC}(t)}{L_b} DT_s \qquad (3)$$

Where t_s and D are the exchanging time frame and obligation cycle of two power switches, separately. The dc-connected capacitor CB provides vitality to C(r), L r and Lm through the switch S1. The capacitor C (0) supplies energy to the LED road-lighting module. At the point when i(Lm) is equivalent to i(Lr), Mode- 2 ends.

Mode 3 [t_4≤t<t_5; see Fig. 8(c)]:

The utility-line voltage Vac and the inductor Lb provide energy to the capacitor Cb through the diode D1, and i(lb) starts to directly diminish at t4.The dc-connected capacitor C_B along with the natural capacitor Cs2 provides vitality to Cr, Lr, and Lm. The capacitor C_0 still supplies vitality to the LED road-lighting module. At the point when Vds2 decreases to zero at t5 Mode- 3 ends.

Mode 4 [t_5≤t<t_6; see Fig. 8(d)]:

At t5, the inductor Lb provides vitality to the capacitor C_B through the diode D5, and i(Lb) linearly diminishes with a down slant of (Vac(t) −Vdc) / Lb. The inductor current i(Lb) is given by

$$i_{Lb}(t) = \frac{v_{AC}(t)}{L_b} DT_s - \frac{V_{DC} - v_{AC}(t)}{L_b} t \qquad (4)$$

The attractive inductor Lm provides vitality to Cr and Lr through the body diode of S2, and to capacitor C (o) along with the LED road-lighting module through diode D4. When S2 turns ON, Mode 4 closes.

Mode 5 [t_6≤t<t_7; see Fig. 8(e)]:

While S2 is ON at t6, Mode 5 begins. The inductor Lb still gives vitality to the capacitor C_B through the diode D5, and i(Lb) linearly diminishes. The inductor Lr provides vitality to Cr through the switch S2, and the attractive inductor Lm provides vitality to capacitor Co along with the LED road-lighting module through diode D4.

At the point when i(Lb) decreases to zero, Mode 5ends.

Mode 6 [t_7≤t<t_8; see Fig. 8(f)]:

At t7, the inductor current i(Lb) is zero. The inductor Lr still provides vitality to C(r) through the switch S2, and the attractive inductor Lm still gives energy to capacitor C_0 along with the LED road-lighting module through diode D4. When i(Lm) reductions to zero, Mode- 6ends.

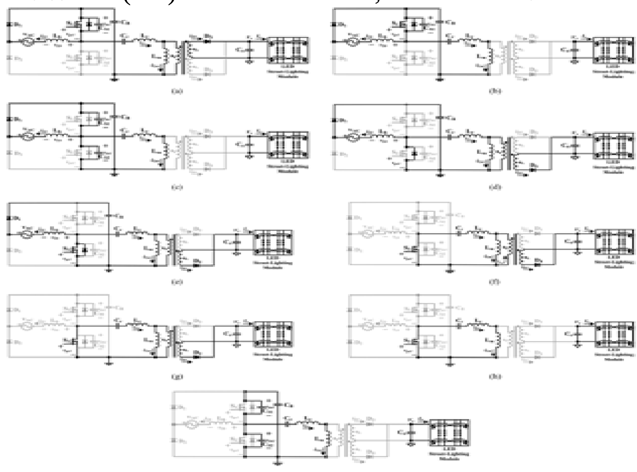

Fig. 8: Operational modes of the displayed single-stage driver for providing an LED road-lighting module.

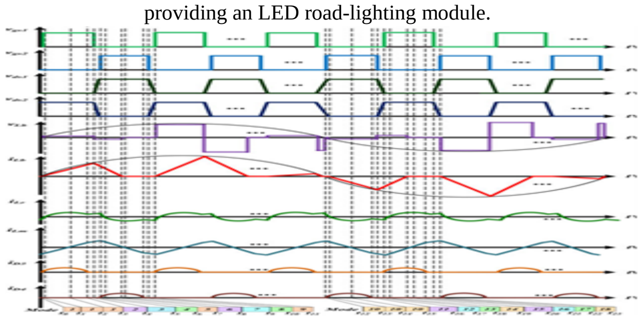

Fig 9: Principle waveforms of the proposed LED driver for road lighting applications.

Mode 7 [t_8≤t<t_9; see Fig. 8(g)]:
The inductor Lr still provides energy to Cr and Lm through the switch S2 , and to capacitor Co along with the LED road-lighting module through diode D4 amid Mode 7. At the point when i(D4) decreases to zero, Mode 7ends.
Mode 8 [t_9≤t<t_10; see Fig. 8(h)]:
At t9, the capacitor Cr gives vitality to Lr and Lm through the switch S2, and the capacitor Co provides vitality to the LED road-lighting module. When S2 skills OFF at t10, Mode 8 ends.
Mode 9 [t_10≤t<t_11; see Fig. 8(i)]:
The capacitors C_{S1} and Cr provide vitality to Lr, Lm, C_{s2} , C_B, and L_{B2} , and the capacitor C(o) still gives vitality to the LED road-lighting module during Mode 9.When vds1 reductions to zero at t_11, Mode 9endsand Mode 1begins again for the following exchanging period. Operational Modes 1–9 perform in the positive half-cycle of info utility-line voltage, while Modes 10–18 occur in the negative half-cycle.

3. DESIGN PROCEDURE FOR THE PROPOSED LED STREET LIGHTING DRIVER

This area exhibits an outline technique for the proposed LED street-lighting driver, and a 144-w-rated LED street-lighting module with 36V/4A yield has been chosen, as an outline case. The outline details are recorded as takes after:

1) Input utility-line voltage (rms esteem):
2) V (ac-rms) =100V (Vac-min)–120V (Vac-max);
3) Input utility-line recurrence: fac = 60 Hz;
4) Rated power of LED street-lighting module: Po = 144 W;
5) Rated voltage of LED street-lighting module: Vo = 36 V;
6) Rated current of LED street-lighting module: Io = 4 A;
7) Estimated efficiency: > 90%.

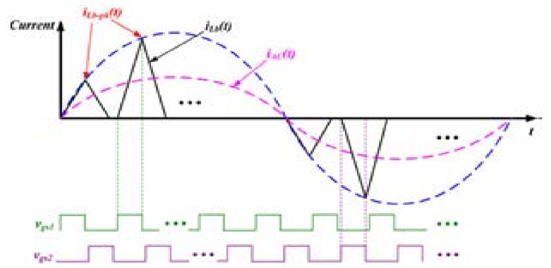

Fig.10: Illustrative waveforms for info utility-line current i_{ac} and inductor current i_{Lb}.

A. Designing The Inductor, L_b:

Fig. 10 demonstrates the illustrative waveforms for information utility-line current i_{ac} and inductor current i_{Lb}. From Fig. 10, value of inductor it can be seen that the pinnacle estimation of inductor current i_{Lb} is equal to the peak value of the utility-line current i_{ac}, and it is acquired as,

$$i_{Lb-pk}(t) = i_{AC-pk}(t) = \frac{\sqrt{2v_{AC-MAX}}\sin(2\pi f_{AC}t)}{L_b} DT_s \quad (5)$$

Where V (ac-max) is the most extreme rms estimation of the info utility line voltage. In every exchange period, the info current i_{ac} (t) is equivalent to the normal estimation of inductor current i(Lb-PK(t)) , and can be communicated by,

$$i_{AC}(t) = \frac{1}{T_s}\int_0^{T_s} i_{Lb-pk}(t).dt = \frac{\sqrt{2}v_{AC-MAX}\sin(2\pi f_{AC}t)D^2T_sV_{DC-MAX}}{2L_b(V_{DC}-\sqrt{2}v_{AC-MAX})} \quad (6)$$

Where V (dc-max)is the greatest dc-transport voltage. Joining (1) with (6), the information normal power is acquired by,

$$P_{in} = \frac{1}{T_{AC}}\int_0^{T_{AC}} v_{AC}(t)i_{AC}(t)dt = \frac{v_{AC-MAX}^2 D^2T_SV_{DC-MAX}}{2L_b(V_{DC}-\sqrt{2}v_{AC-MAX})} \quad (7)$$

Where t_{ac} is a utility-line cycle.

The appraised yield power Po of the LED road-lighting module is related with information control Pin and is given by,

$$P_0 = \eta P_{in} = \frac{v_{AC-MAX}^2 D^2T_SV_{DC-MAX}}{2L_b(V_{DC}-\sqrt{2}v_{AC-MAX})} \quad (8)$$

Where η is the assessed effectiveness of the driver circuit. Improving (8), the outline condition of the inductor L_b is given by

$$L_b = \frac{\eta v_{AC-MAx}^2 D^2V_{DC-MAX}}{2P_0f_S(V_{DC}-\sqrt{2}v_{AC-MAX})} \quad (9)$$

With a η of 0.9, a D of 0.5, a Po of 144 W, an exchanging frequency fs of 120 kHz, a V (ac-max) of 120 V and assuming a V (dc-max) of 340 V, the inductor Lb is given by,

$$L_b = \frac{0.9.120^2.0.5^2.340}{2.144.120k(340-120\sqrt{2})} \cong 188\mu H$$

B. Figuring the Minimum Dc-Bus Voltage V_{DC}:

Referring to (8), the minimum dc-bus voltage V_{DC-MIN} with respect to the minimum input utility-line voltage V_{DC-MIN} can be expressed by,

$$V_{DC-MIN} = \frac{2\sqrt{2}L_bP_0v_{AC-MAX}}{2L_bP_0-\eta T_SD^2v_{AC-MIN}^2} \quad (10)$$

With an inductor Lb of 188 μH, the voltage V_{DC-MIN} is calculated by

$$V_{DC-MIN} = \frac{2\sqrt{2}.188\mu.144.100}{2.188\mu.144-0.9.\left(\frac{1}{120k}\right).0.5^2100^2} = 216.3V$$

C. Deciding the Transformer Turns Ratio "N":

The turns-ratio n of transformer T_1 is given as,

$$n = \frac{n_p}{n_s} \geq \frac{DV_{DC-MAX}}{V_0+V_F} \quad (11)$$

Where Vf is the forward voltage drop of the yield rectifier diodes D3 and D4, and Vo is the yield voltage.
With a Vo of 36 V and a Vf of 0.7 V, the turns proportion **n** is given by,

$$n = \frac{n_p}{n_s} \geq \frac{0.5.340}{36+0.7} = 4.6$$

Calculating the Equivalent Load Resistance, Req

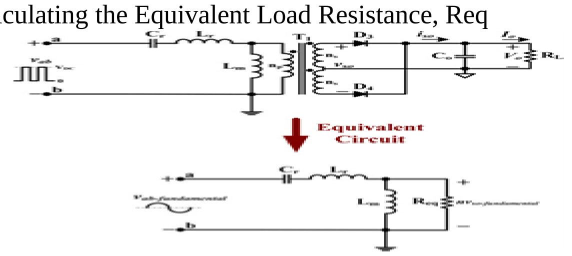

Fig. 11: Original circuit chart and its proportional circuit of the LLC full system.

Fig. 11 shows the first circuit outline and its comparable circuit of the LLC resounding system, where Vab is the input square waveform with a greatness of Vdc, which can be obtained by on the other hand, directing the power switches S1 and S2; Vso and i_{so} are yield voltage and current, individually, in the optional side of transformer T_1. The major parts of the voltage Vab can be communicated by,

$$v_{ab-fun\,damental} = \frac{2}{\pi} V_{DC} \sin \omega_S t \quad (12)$$

Where ω_s is the exchanging frequency. The central segments of voltage Vso, meant as Vso fundamental, and current i_{so} in the optional side of transformer T1 are, separately, acquired by,

$$v_{s0-fundamental} = \frac{4}{\pi} V_0 \sin \omega_S t, \quad (13)$$

and

$$i_{s0} = \frac{\pi}{2} I_0 \sin \omega_s t \quad (14)$$

Utilizing (13) and (14), the identical load resistance Req that is referred to the essential side of transformer T1 can be communicated as,

$$R_{eq} = n^2 \frac{u_{s0-fundamental}}{i_{s0}} = \frac{8n^2 V_0}{\pi^2 I_0} = \frac{8n^2}{\pi^2} R_L \quad (15)$$

Where R_L is the proportional resistance of the LED road-lighting module, and which can be spoken to by R_L=Vo/Io With a transformer proportion **n** of 4.6 acquired from (11), the identical load resistance Req is given by,

$$R_{eq} = \frac{8n^2}{\pi^2} R_L = \frac{8.4.6^2}{\pi^2}\left(\frac{36}{4}\right) = 154.4\Omega$$

Determining the Maximum and Minimum Voltage Gain of the LLC Resonant Network:

Referring to the *LLC* resonant network shown in Fig. 9, the Quality factor Q_r is defined as,

$$Q_r = \frac{\sqrt{L_r}}{R_{eq}\sqrt{C_r}} \quad (16)$$

The primary resounding frequency ω_{r1} and optional resonant frequency ω_{r2} of the LLC thunderous system are, separately, characterized as ,

$$\omega_{r1} = 2\pi f_{r1} = \frac{1}{\sqrt{L_r C_r}} \quad (17)$$

and

$$\omega_{r2} = 2\pi f_{r2} = \frac{1}{\sqrt{(L_m + L_r) C_r}} \quad (18)$$

The inductance proportion A is characterized as,

$$A = \frac{L_m}{L_r} \quad (19)$$

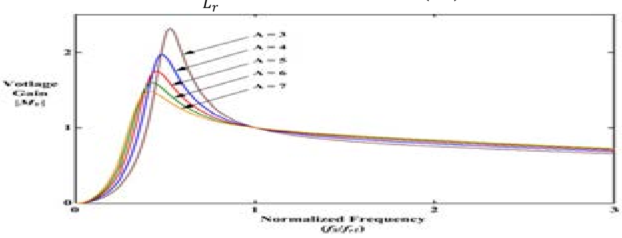

Fig. 12: Voltage gain |MV | of the LLC resonant converter versus normalized frequency f_s/f_{r1} under different inductance ratios (Q_r= 0.3).

By utilizing the major guess strategy, the voltage pick up |MV | of the LLC full system is gotten as,

$$|M_V(\omega_S)| = \frac{n v_{so-fundamental}}{v_{ab-fund\,amental}} = \frac{n\frac{4V_0}{\pi}\sin \omega_S t}{\frac{2}{\pi} V_{DC} \sin \omega_s t} = \frac{2n.V_0}{V_{DC}} \quad (20)$$

$$= \left| \frac{A\left(\frac{\omega_s}{\omega_{r1}}\right)^2}{\left[(A+1)\left(\frac{\omega_s}{\omega_{r1}}\right)^2 - 1\right] + j\,Q_r A\left(\frac{\omega_s}{\omega_{r1}}\right)\left[\left(\frac{\omega_s}{\omega_{r1}}\right)^2 - 1\right]} \right| \quad (21)$$

At the point when the exchanging recurrence ω_s is chose to be equalto the principle thunderous frequency ω_{r1}, the base voltage gain M_{V-MIN}, which happens in the most extreme dc-transport voltageV_{DC-MAX}, is gotten as ,

$$M_{V-MIN} = |M_V(\omega_s)|_{\omega_s=\omega_{r1}} = 1 \quad (22)$$

Then again, the most extreme voltage gain M_{V-MIN}, occurring in the base dc-transport voltageV_{Dc-MIN}, is expressed as,

$$M_{V-MAX} = \frac{V_{DC-MAX} . M_{V-MIN}}{V_{DC-MIN}} \quad (23)$$

With a V_{DC-MAX} of 340 V and a V_{DC-MIN} of 216.3 V, theM_{V-MAX} is got by

$$M_{V-MAX} = \frac{340.1}{216.3} = 1.57$$

A. Determining the Inductance Ratio A

In this plan case, the fundamental thunderous frequency f_{r1} and quality figure Q_r are chose to be 120 kHz (the same as the switching recurrencef_s) and 0.3, individually. Agreeing to (20), fig. 2.8 demonstrates the relationship between voltage pick up $|M_v|$and standardized frequency f_s/f_{r1}under various inductanceratios. Alluding to fig.2.8. Furthermore, with thought given to the required greatest and least voltage picks up | $|M_v|$of the LLC full system, which are 1.57 and 1, the inductance proportion A is reasonably chosen to be 5 in this outline case. Also, substituting (19) into (17) and (18), the auxiliary full frequency $f_{r2}$is given by,

$$f_{r2} = \sqrt{\frac{f_{r1}^2}{A+1}} \quad (24)$$

With an fr1 of 120 kHz and an A of 5, the auxiliary full recurrence fr2 is figured by,

$$f_{r2} = \sqrt{\frac{(120k)^2}{5+1}} \cong 49kHZ$$

B. Designing the LLC Resonant Network

Isolating (16) by (17), the inductor *Lr* can be communicated by,

$$L_r = \frac{Q_r R_{eq}}{2\pi f_{r1}} \quad (25)$$

From (19), the attractive inductor L_m is given by,

$$L_m = AL_r \quad (26)$$

The full capacitor C_r can be acquired by,

$$C_r = \frac{1}{(2\pi f_{r1})^2 L_r} \quad (27)$$

With an f_{r1} of 120 kHz, an R_{eq} of 154.4 Ω, an A of 5 and a Q_r of 0.3, the LLC full system separately, given by,

$$L_r = \frac{Q_r R_{eq}}{2\pi\pi f_{r1}} = \frac{0.3.154.4}{2\pi, 120k} = 61.4\mu H$$

$$L_m = AL_r = 5.61.4\mu = 307\mu H,$$

$$C_r = \frac{1}{(2\pi f_{r1})^2 L_r} = \frac{1}{(2\pi.120k)^2 . 61.4\mu} = 28.6nf$$

Also, the inductors $L_r$and L_m, and capacitor $C_r$are choose as 60 μH, 300 μH, and 33 nF, separately.

4. SIMULATION RESULTS

In this paper, the proposed model is designed and simulated in software called MATLAB/SIMULATION. The figures shows that the performance of the novel single stage light emitting diode driver for street lighting applications.

A. Existing system Results:

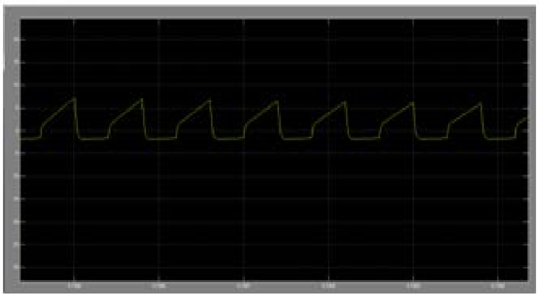

Fig 13.1. Measured inductor current iLb (2 A/div); time scale: 2 µs/div.

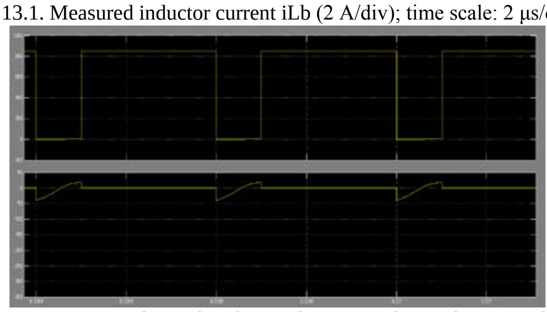

Fig 13.2. Measured switch voltage vds2 (200V/div) and current ids2 (2A/div); time scale: 2 µs/div.

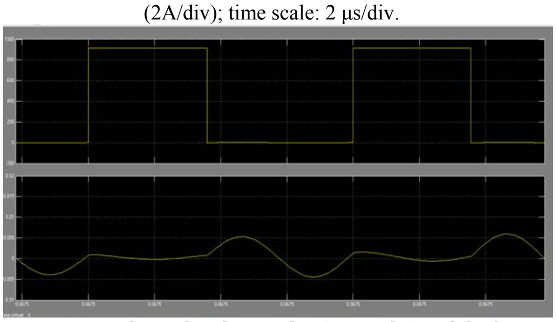

Fig 13.3. Measured switch voltage Vds1 (200 V/div) and diode current iD3 (5 A/div); time scale: 2 µs/div.

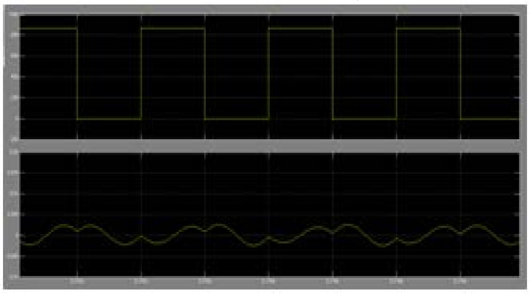

Fig 13.4. Measured switch voltage Vds2 (200 V/div) and resonant current iLr (2 A/div); time scale: 2 µs/div.

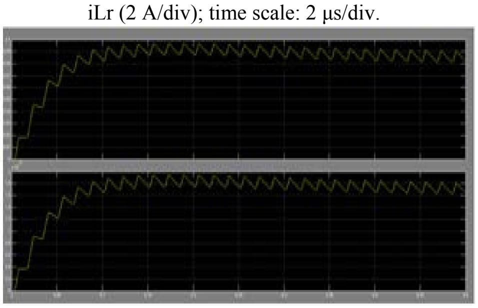

Fig 13.5. Measured output voltage Vo (10V/div) and current Io (2A/div); time scale: 5 ms/div.

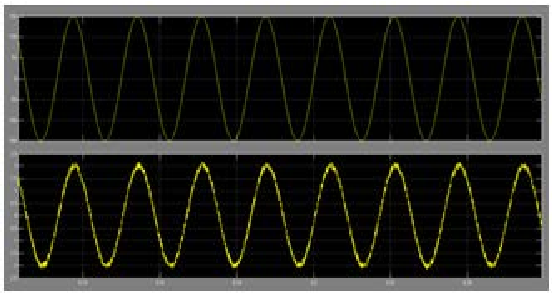

Fig 13.6. Measured input utility-line voltage VAC (50 V/div) and current iac (2 A/div); time scale: 5 ms/div.

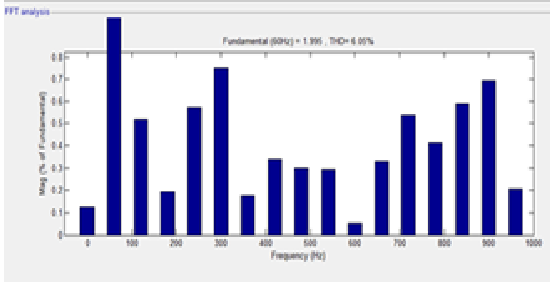

Fig 13.7. THD of current.

B. Proposed System Results:

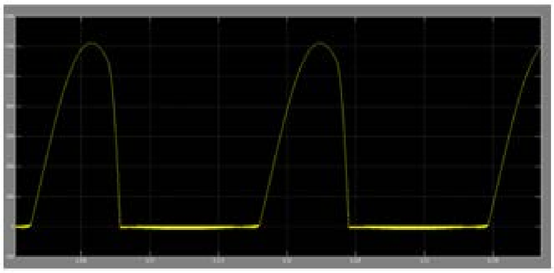

Fig 14.1. Proposed measured inductor current iLb (2 A/div); time scale: 2 µs/div.

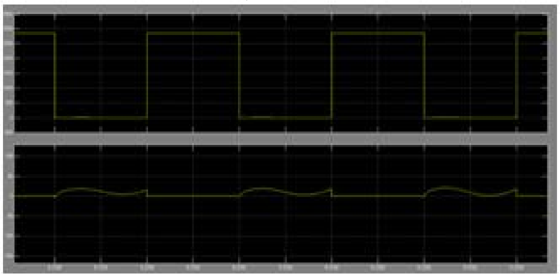

Fig 14.2. Proposed measured switch voltage vds2 (200V/div) and current ids2 (2A/div); time scale: 2 µs/div.

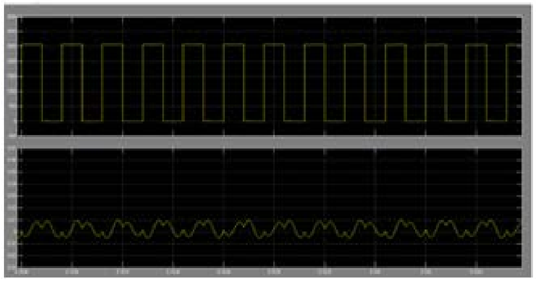

Fig 14.3. Proposed measured switch voltage Vds1 (200 V/div) and diode current iD3 (5 A/div); time scale: 2 µs/div.

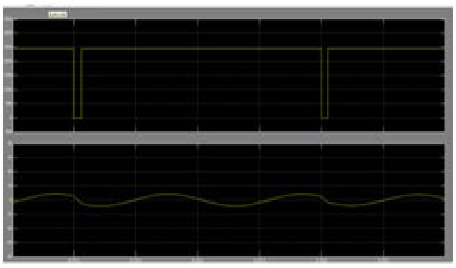

Fig 14.4. Proposed measured switch voltage Vds2 (200 V/div) and resonant current iLr (2 A/div); time scale: 2 µs/div.

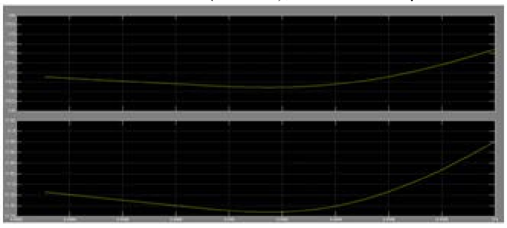

Fig 14.5. Proposed measured output voltage Vo (10V/div) and current Io (2A/div); time scale: 5 ms/div.

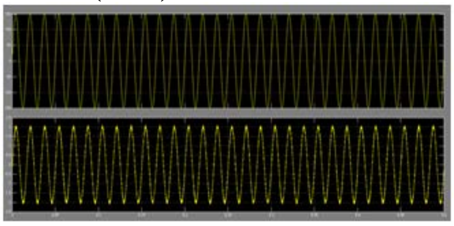

Fig 14.6. Extension measured input utility-line voltage VAC (50 V/div) and current iac (2 A/div); time scale: 5 ms/div.

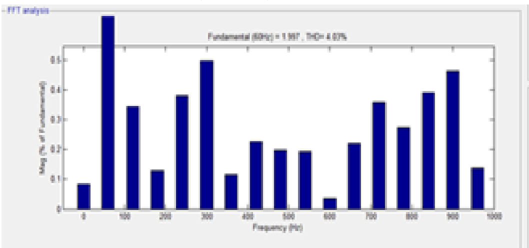

Fig 14.7 Proposed THD of current.

5. CONCLUSION

The control objectives had been analyzed and it is concluded that the control loop must provide accurate phase and amplitude regulation of the power in the ripple-port. Thus a current control loop with PR controller is proposed for the ripple-port. In addition, an 80 feed-forward control, including amplitude calculation and phase-locked-loop, is added between the AC/DC converter and the ripple-port. A circuit topology with Boost PFC regulator as the AC/DC stage and an H-bridge inverter as the ripple-port is chosen as an example to illustrate the design of a ripple-port integrated rectifier. The discussion was focused on the ripple-port design and the interaction between the ripple-port and the PFC regulator. In the design example, it is illustrated how to design the decoupling capacitor in the ripple-port to achieve minimum capacitance and to optimize efficiency. A loss model is derived to show how to choose the operating point of the ripple-port, including switching frequency, voltage swing and inductor sizing.

6. FUTURE SCOPE

The extension of this work might focus on the following aspects:

- Feedback control of the dc-link voltage ripple.
- The response of the dc-link voltage ripple is not monotonic to the control signal, therefore the feedback control requires comparison between the present state and the previous state to decide whether to increase or decrease the control signal, similar to the MPPT algorithm.
- Optimize the hardware design to achieve high efficiency.
- Compare the efficiency between continuous conduction mode (CCM), discontinuous conduction mode (DCM) and critical conduction mode (CRM) operation of the ripple-port. Then choose the optimal operating mode.
- In Future we can implement fuzzy /adaptive artificial neural network concepts.

REFERENCES:

[1] E. F. Schubert, Light-Emitting Diodes. Cambridge, U.K.: Cambridge Univ. Press, 2006.

[2] C. L. Kuo, T. J. Liang, K. H. Chen, and J. F. Chen, "Design and implementation of high frequency AC-LED driver with digital dimming," in Proc. IEEE Int. Symp. Circuit Syst., 2010, pp. 3713–3716.

[3] C. S. Moo, Y. J. Chen, and W. C. Yang, "An efficient driver for dimmable LED lighting," IEEE Trans. Power Electron., vol. 27, no. 11, pp. 4613–4618, Nov. 2012.

[4] R. L. Lin, Y. C. Chang, and C. C. Lee, "Optimal LED array combination for single-loop CCM buck-boost driver," IEEE Trans Ind. Appl., vol. 49, no. 2, pp. 761–768, Mar./Apr. 2013.

[5] H. J. Chiu and S. J. Cheng, "LED backlight driving system for large-scale of LCD panels," IEEE Trans Ind. Electron., vol. 54, no. 5, pp. 2751–2760, Oct. 2007.

[6] J. M. Alonso, J. Vina, D. G. Vaquero, G. Martinez, and R. Osorio, "Analysis and design of the integrated double buck-boost converter as a high power-factor driver for power-LED lamps," IEEE Trans. Ind. Electron., vol. 59, no. 4, pp. 1689–1697, Apr. 2012.

[7] K. I. Hwu, Y. T. Yau, and L. L. Lee, "Powering LED using high-efficiency SR fly back converter," IEEE Trans Ind. Appl., vol. 47, no. 1, pp. 376–386, Jan./Feb. 2011.

[8] S. Y. R. Hui and Y. X. Qin, "General photo-electro-thermal theory for light-emitting diodes (LED) systems," IEEE Trans. Power Electron., vol. 24, no. 8, pp. 1967–1976, Aug. 2009.

[9] G. Sauerlander, D. Hente, H. Radermacher, E. Waffen schmidt, and J. Jacobs, "Driver electronics for LEDs," in Proc. IEEE Ind. Appl. Soc. Annu. Meeting, 2006, pp. 2621–2626.

[10] Y. S. Chen, T. J. Liang, K. H. Chen, and J. N. Juang, "Study and implementation of high frequency pulse LED driver with self-oscillating circuit," in Proc. IEEE Int. Symp. Circuit Syst., 2011, pp. 498–501.

[11] Y. J. Chen, W. C. Yang, C. S. Moo, and Y. C. Hsieh, "A high efficiency driver for high-brightness white LED lamp," in Proc. IEEE TENCON Conf., 2010, pp. 2313–2317.

[12] C. Y. Wu, T. F. Wu, J. R. Tsai, Y. M. Chen, and C. C. Chen, "Multi string LED backlight driving system for LCD panels with color sequential display and area control," IEEE Trans. Ind. Electron., vol. 55, no. 10, pp. 3791–3800, Oct. 2008.

[13] S. Y. R. Hui, S. N. Li, X. H. Tao, W. Chen, and W. M.Ng, "A novel passive off-line light-emitting diode (LED) driver with long lifetime," IEEE Trans. Power Electron., vol. 25, no. 10, pp. 2665–2672, Oct. 2010.

[14] LED lighting solutions. ON Semiconductor. pp. 1–48. Mar. 2013. [Online]. Available: http://www.onsemi.cn /pub link/Collateral/BRD8034-D.PDF.

[15] D. G. Lamar, J. S. Zuniga, A. R. Alonso, M. R. Gonzalez, and M. M. Hernando, "A very simple control strategy for power factor corrections driving high-brightness LEDs," IEEE Trans. Power Electron., vol. 24, no. 8, pp. 2032–2042, Aug. 2009.

[16] Energy-efficient solutions for offline LED lighting and general illumination. STMicroelectronics Brochure. Pp.1-27. [Online]. Available: http://www.mouser.com/pdf Docs /STMicro_OFFLINEGENERAL_ILLUMINATION_A.pdf.

[17] M. Arias, D. G. Lamar, F. F. Linera, D. Balocco, A. A. Diallo, and J. Sebastian, "Design of a soft-switching asymmetrical half-bridge converter as second stage of an LED driver for street lighting application," IEEE Trans. Power Electron., vol. 27, no. 3, pp. 1608–1621, Mar. 2012.

[18] M. Arias, D. G. Lamar, J. Sebastian, D. Balocco, and A. Diallo, "High efficiency LED driver without electrolytic capacitor for street lighting," IEEE Trans Ind. Appl., vol. 49, no. 1, pp. 127–137, Jan./Feb. 2013.

[19] X. Long, R. Liao, and J. Zhou, "Development of street lighting system based novel high-brightness LED modules," IET Optoelectron., vol. 3, no. 1, pp. 40–46, Feb. 2009.

[20] C. A. Cheng, H. L. Cheng, C. H. Chang, F. L. Yang, and T. Y. Chung, "A single-stage LED driver for street-lighting applications with interleaving PFC feature," in Proc. IEEE Int. Symp. Next-Generation Electron. 2013, pp. 150–152.

[21] High-pressure sodium lamps- VIALOX NAV-E technical information, OSRAM, pp. 1–6. [Online]. Available: http://www.osram.com/media/resource/hires/343306/family-vialox-nav-e.pdf.

[22] 10000Lm LED Street Light Specification Model No. LM9003–003G/GT, AcBel Polytech, Inc., pp. 1–10, 2010. [Online]. Available: http://www.acbel.com/ProductFile/ SPEC-LM9003–003G_GT(eng).pdf.

[23] S. C. Huang, L. L. Lee, M. S. Jeng, and Y. C. Hsieh, "Assessment of energy-efficient LED street lighting through large-scale demonstration," in Proc. Int. Conf. Renewable Energy Res. Appl., 2012, pp. 1–5.

[24] C. C. Lin, L. S. Yang, and E. C. Chang, "Study of a DC-DC converter for solar LED street lighting," in Proc. IEEE Int. Symp. Next-Generation Electron. 2013, pp. 461–464.

[25] G. C. Jane, C. C. Su, H. J. Chiu, and Y. K. Lo, "High-efficiency LED driver for street light applications," in Proc. Int. Conf. Renewable Energy Res. Appl., 2012, pp. 1–5.

[26] C. Spini, "AN3106-48V-130W high-efficiency converter with PFC for LED street lighting applications," ST Micro electron. Appl. Note, pp. 1–34, Sep. 2012.

[27] S. Hu. (2010, Nov.). 200 W AC/DC LED drivers. Texas Instruments. [Online]. pp. 1–4. http://www.ti.com/lit/ml/ slur086/slur086.pdf.

[28] R. L. Steigerwald, "A comparison of half-bridge resonant converter topology," IEEE Trans. Power Electron., vol. 3, no. 2, pp. 174–182, Apr. 1988.